

## Pre-Compression Volume on Flow Ripple Reduction of a Piston Pump

XU Bing\*, SONG Yuechao, and YANG Huayong

State Key Lab of Fluid Power and Mechatronic System, Zhejiang University, Hangzhou 310027, China

Received October 11, 2012; revised July 9, 2013; accepted September 9, 2013

**Abstract:** Axial piston pump with pre-compression volume(PCV) has lower flow ripple in large scale of operating condition than the traditional one. However, there is lack of precise simulation model of the axial piston pump with PCV, so the parameters of PCV are difficult to be determined. A finite element simulation model for piston pump with PCV is built by considering the piston movement, the fluid characteristic(including fluid compressibility and viscosity) and the leakage flow rate. Then a test of the pump flow ripple called the secondary source method is implemented to validate the simulation model. Thirdly, by comparing results among the simulation results, test results and results from other publications at the same operating condition, the simulation model is validated and used in optimizing the axial piston pump with PCV. According to the pump flow ripples obtained by the simulation model with different PCV parameters, the flow ripple is the smallest when the PCV angle is  $13^\circ$ , the PCV volume is  $1.3 \times 10^{-4} \text{ m}^3$  at such operating condition that the pump suction pressure is 2 MPa, the pump delivery pressure 15 MPa, the pump speed 1 000 r/min, the swash plate angle  $13^\circ$ . At the same time, the flow ripple can be reduced when the pump suction pressure is 2 MPa, the pump delivery pressure is 5 MPa, 15 MPa, 22 MPa, pump speed is 400 r/min, 1 000 r/min, 1 500 r/min, the swash plate angle is  $11^\circ$ ,  $13^\circ$ ,  $15^\circ$  and  $17^\circ$ , respectively. The finite element simulation model proposed provides a method for optimizing the PCV structure and guiding for designing a quieter axial piston pump.

**Key words:** pre-compression volume, flow ripple, operating condition, axial piston pump

### 1 Introduction

The noise is a disadvantage to the extension of application of the axial piston pump in a low-noise limit environment. It is accepted by most researchers that there are two main different styles of noise: the fluid-borne and structure-borne noise. As the main causing of fluid-borne noise, the flow ripple has drawn much attention.

The existing pump flow ripple reduction methods are given in Fig. 1.

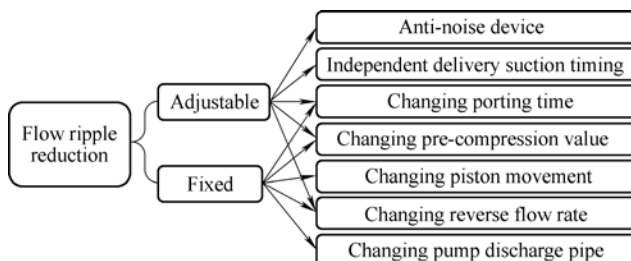


Fig. 1. Methods for reducing pump flow ripple

Based on Fig. 1, it can be seen that there are two different pump flow-ripple reduction methods: the fixed and adjustable method. The fixed methods (such as relief

groove and relief bore) work very well under certain operating conditions, but when the operating conditions change, the pump noise may increase greatly. Therefore, the adjustable methods such as compensating for pump flow ripple with servo valve, changing port time with check valve have been developed. There is also a method which can be classified both into the fixed and the adjustable method called pre-compression volume method, if the structure of pre-compression volume is variable during the operation of piston pump, the method is adjustable, if not, the method is fixed. Some typical reduction methods are depicted in details as following.

#### (1) Relief groove and relief bore

The relief groove and relief bore, a traditional method that compresses the oil in the cylinder chamber by introducing the oil from the pump delivery port, has been investigated by many researchers. In 2003, MANRING, et al<sup>[1]</sup>, analyzed the principal advantages of the relief groove with various geometries. In 2004, IVANTYSNOVA, et al<sup>[2]</sup>, gave a method to compute the relief-groove smallest cross section called AVAS. This method is simple, but is very sensitive to operating conditions.

#### (2) Cross angle

This method can be achieved by rotating the swash plate around the axis that perpendicular synchronously to both the axis along the shaft and the axis that the swash plate rotates around for generating the swash plate angle. In 2004,

\* Corresponding author. E-mail: bxu@zju.edu.cn

This project is supported by National Key Technology R&D Program of the Eleventh Five-year Plan of China(Grant No. 2011BAF09B03), and National Natural Science Foundation of China(Grant No. 51075360)

© Chinese Mechanical Engineering Society and Springer-Verlag Berlin Heidelberg 2013

MANRING, et al<sup>[3]</sup> analyzed the impact of secondary angle (named cross angle) of the swash plate on flow ripple, force and torque. The main conclusion is that the secondary angle of the swash plate reduces the flow ripple in large scale of operating conditions. However, the magnitude of the required control-effort for the pump is increased, and a new requirement of containment to control the secondary angle is needed. In 2005, ERICSON<sup>[4]</sup> provided experimental results of flow ripple generated by cross angle. It can be inferred that the method is useful in reducing flow ripple in some operating conditions but the setup is so complicated that it is impracticable to be used in industrial.

(3) Compensating for pump flow ripple with servo valve

It is a method that the pump flow ripple is reduced by compensating it with another flow ripple, which the phase is opposite with the pump flow ripple and the amplitude is the same. In 2008, WANG, et al<sup>[5]</sup>, gave a method to attenuate the fluid-born noise method, in which a high frequency servo valve was used to generate the compensating flow ripple. It can be concluded that the method reduces flow ripple only in narrow-band frequency scale, due to the lower frequency of the servo valve. In addition, the method costs too much.

(4) Changing porting time with check valve

Through changing the porting time (the time that the cylinder chamber connect to the pump delivery/suction port), the flow ripple of the pump can be reduced as small as possible in theory. This method can be reached by rotating the port plate or changing the open time of check valve. In 2008, TIMO, et al<sup>[6]</sup>, analyzed the open time of the check valve, and it can be seen that this method can reduce both the flow ripple and swash plate torque. However, due to limitation of the check valve frequency and life, this method is not succeed to be used in industrial application.

(5) PCV method

The Pre-Compression Volume method can reduce flow ripple in large scale of operating conditions with a blocked volume or an adjustable volume connected to Bottom Dead Center of the port plate. In 1991, PETERSSON, et al<sup>[7]</sup>, investigated the pre-compression filter volume(PCFV), and it can be concluded that the reverse flow rate was reduced after introducing PCFV. In 2006, SEENIRAJ, et al<sup>[8]</sup>, researched the effect of PCFV on flow ripple and cylinder pressure, and it can be concluded that the flow ripple of piston pump is reduced greatly under most operating conditions when the PCFV Volume is  $7.5 \times 10^{-5} \text{ m}^3$ .

Although several researchers have paid their attention on PCV method, almost all models for piston pump with PCV are using lumped parameter method; there is neither accuracy model for analyzing the structure of PCV nor appropriate method to determine the parameters of the PCV for a typical piston pump. So a finite element model for piston pump with PCV is proposed and the parameters selection method for PCV is established in this paper. In

addition, the effect of the PCV on flow ripples under different pump delivery pressure, pump speed and swash plate angle is analyzed.

## 2 Simulation Model of Axial Piston Pump

### 2.1 Operational principle of PCV

The flow ripple is influenced by kinematic flow rate and dynamic flow rate<sup>[9]</sup>. The dynamic flow rate occurs due to the pressure difference between the cylinder chamber and the suction/delivery port, it is the reverse flow rate around the bottom dead center(BDC) that influences remarkably the flow ripple<sup>[10-11]</sup>. Therefore, it is a better way to reduce the generation of reverse flow rate around BDC in order to reduce the flow ripple.

The operational principle of PCV is shown in Fig. 2.

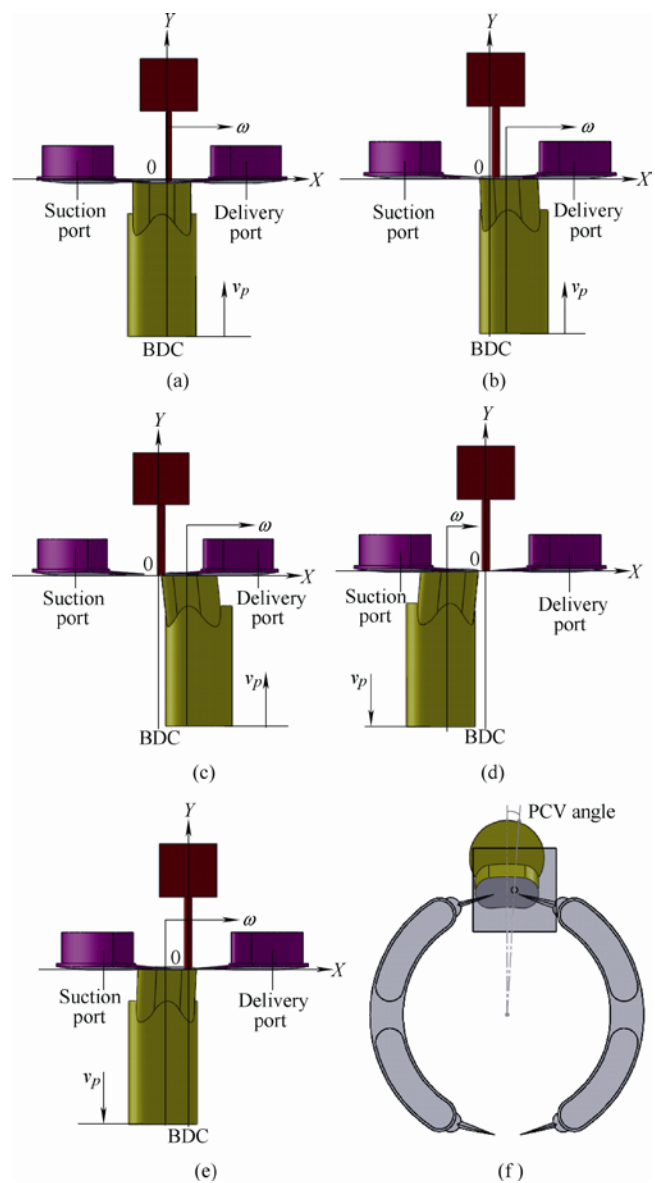


Fig. 2. Operational principle of PCV Methods

When the piston locates at the BDC as shown by Fig. 2(a), the piston speed in y direction is zero, and the pressure in delivery port and PCV are larger than in the

cylinder chamber, so the fluid flows from the delivery port and PCV into the cylinder chamber.

As the piston moving, the piston moves in y direction as shown in Fig. 2(b). Because the pressure in PCV is larger than that in the cylinder chamber, the fluid flows from PCV into the cylinder chamber. The pump delivery pressure is higher than that in the cylinder chamber, so the fluid flows into the cylinder chamber. In other words, the reverse flow rate occurs.

The piston rotates around y negative direction as shown in Fig. 2(c), the piston continues moving in y direction. When the pressure in cylinder chamber is larger than or equal to that in PCV and delivery port, the fluid flows out of the cylinder chamber into the delivery port and PCV.

When the piston leaves away the suction port as shown in Fig. 2(d), the piston moves in the opposite y direction, and the fluid flows from suction port to cylinder chamber.

As the piston connecting to the PCV and suction port, as shown in Fig. 2(e), the piston moves at opposite y direction, so the fluid flows from suction port to cylinder chamber. In addition, when the pressure in PCV is larger than that in cylinder chamber, the fluid flows from the PCV into the cylinder chamber.

According to the depiction mentioned above, it can be seen that the reverse flow rate from the delivery port is reduced, because additional fluid flows into the cylinder chamber from the PCV. Therefore, it is reasonable to infer that the pump discharge flow ripple is reduced.

### 2.2 CFD model

The simulation model is computed by Fluent, and the fluid in the pump is shown in Fig. 3.

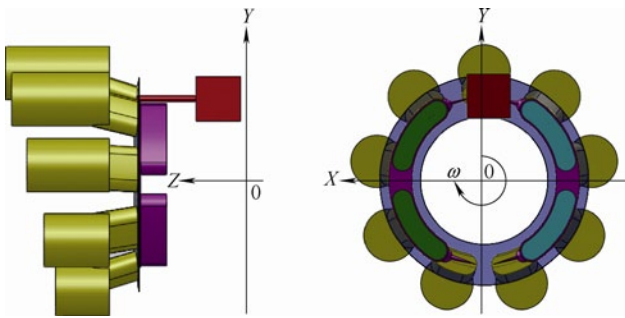


Fig. 3. Fluid in the piston pump

Govern equation: The finite volume method is adopted by Fluent to compute conservation equations of mass, momentum and energy in every control volume.

The conservation equation of mass<sup>[12]</sup>:

$$\frac{\partial \rho}{\partial t} + \frac{\partial \rho u}{\partial x} + \frac{\partial \rho v}{\partial y} + \frac{\partial \rho w}{\partial z} = S_m. \quad (1)$$

The conservation equation of momentum:

$$\frac{\partial(\rho u)}{\partial t} + \frac{\partial(\rho uu)}{\partial x} + \frac{\partial(\rho uv)}{\partial y} + \frac{\partial(\rho uw)}{\partial z} =$$

$$\begin{aligned} & -\frac{\partial p}{\partial x} + \frac{\partial}{\partial x} \left( \mu \frac{\partial u}{\partial x} \right) + \frac{\partial}{\partial y} \left( \mu \frac{\partial u}{\partial y} \right) + \frac{\partial}{\partial z} \left( \mu \frac{\partial u}{\partial z} \right) + S_u, \\ & \frac{\partial(\rho v)}{\partial t} + \frac{\partial(\rho vu)}{\partial x} + \frac{\partial(\rho vv)}{\partial y} + \frac{\partial(\rho vw)}{\partial z} = \\ & -\frac{\partial p}{\partial x} + \frac{\partial}{\partial x} \left( \mu \frac{\partial v}{\partial x} \right) + \frac{\partial}{\partial y} \left( \mu \frac{\partial v}{\partial y} \right) + \frac{\partial}{\partial z} \left( \mu \frac{\partial v}{\partial z} \right) + S_v, \quad (2) \\ & \frac{\partial(\rho w)}{\partial t} + \frac{\partial(\rho wu)}{\partial x} + \frac{\partial(\rho wv)}{\partial y} + \frac{\partial(\rho ww)}{\partial z} = \\ & -\frac{\partial p}{\partial z} + \frac{\partial}{\partial x} \left( \mu \frac{\partial w}{\partial x} \right) + \frac{\partial}{\partial y} \left( \mu \frac{\partial w}{\partial y} \right) + \frac{\partial}{\partial z} \left( \mu \frac{\partial w}{\partial z} \right) + S_w. \end{aligned}$$

The conservation equation of energy:

$$\begin{aligned} & \frac{\partial(\rho T)}{\partial t} + \frac{\partial(\rho u T)}{\partial x} + \frac{\partial(\rho v T)}{\partial y} + \frac{\partial(\rho w T)}{\partial z} = \\ & \frac{\partial}{\partial x} \left( \frac{k}{c_p} \frac{\partial T}{\partial x} \right) + \frac{\partial}{\partial y} \left( \frac{k}{c_p} \frac{\partial T}{\partial y} \right) + \frac{\partial}{\partial z} \left( \frac{k}{c_p} \frac{\partial T}{\partial z} \right) + S_T. \quad (3) \end{aligned}$$

The flow state around the relief groove of the port plate is turbulence, and the other region is laminar flow. Due to the little influence of the flow state on the pump discharge flow ripple, the turbulence is ignored.

Kinematic flow rate: As one of the main influencing factors, the kinematic flow rate (generated by the piston movement) is computed by the following equations.

The rotation speed  $\omega$ :

$$\omega = \frac{2\pi n}{60}; \quad (4)$$

the reciprocating speed  $v_p$ :

$$v_p = R\omega \sin \phi \tan \beta. \quad (5)$$

Fluid characteristic: Because the fluid compressibility has an important influence in flow ripple, it is considered in the simulation model. The fluid density  $\rho$  is calculated by the following equation:

$$\rho = \frac{\rho_0}{1 - (p - p_0)/K}, \quad (6)$$

the sound velocity  $c_0$  is computed by

$$c_0 = \sqrt{\frac{K}{\rho}} = \sqrt{\frac{K - (p - p_0)}{\rho_0}}. \quad (7)$$

Leakage flow rate: The magnitude of leakage flow rate is almost the same with the reverse flow rate, so it is reasonable to conclude that the leakage flow rate exerts an important influence on flow ripple. The fluid viscosity affects leakage flow rate considerably, so it must be

modeled exactly by<sup>[10]</sup>

$$\eta = 0.0457 \exp \left\{ 6.58 \times \left[ \left( 1 + 5.1 \times 10^{-9} p \right)^{2.3 \times 10^{-8}} \times \left( \frac{T - 138}{303 - 138} \right)^{-1.16} - 1 \right] \right\} \quad (8)$$

The extra-thin oil film(0.005 mm–0.03 mm) is used to compute the leakage flow rate in CFD model for piston pump.

Due to the large length difference between the oil film and the other component, the interval size of the grid around the oil film is set to the same value, and the largest proportion of the grid interval size in the simulation model should be less than 3. For increase the computation accuracy, the time step is set to be less than  $6 \times 10^{-5}$  s, and the number of the time step should be more than 1 000.

### 2.3 Boundary condition

To obtain precise simulation result, it is needed to determine appropriate boundary condition. The pump delivery port and the oil-film edge are set to be the pressure outlet, and the pump suction port is set to be the pressure inlet.

Based on pump operational principle, the piston movement is modeled by sliding and dynamic mesh, which is shown in Fig. 4.

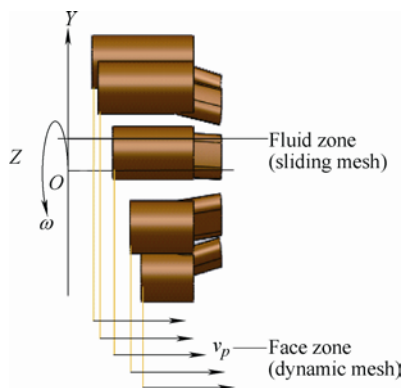


Fig. 4. Movement setting of the fluid

Some parameters of the simulation model are given in Table 1.

Table 1. Parameters of simulation model

Fluid density $\rho_0 / (\text{kg} \cdot \text{m}^{-3})$	Fluid viscosity $\mu_0 / (\text{kg} \cdot \text{m} \cdot \text{s}^{-1})$	Reference pressure $p_0 / \text{MPa}$	Number of piston $Z$	Pitch circle $R / \text{mm}$
871	0.048	1.013	9	73.5
Reference temperature $T_0 / \text{K}$	Temperature in discharge/suction port $T_m \& T_{out} / \text{K}$		Temperature at leakage region $T_l / \text{K}$	
300	313.75		333.75	

## 3 Simulation Model Validation

In this section, the test results under different operation

conditions are provided to validate the simulation model.

### 3.1 Test principle and apparatus

The Secondary Source Method is adopted to test the pump flow ripple, and the schematic diagram is shown in Fig. 5.

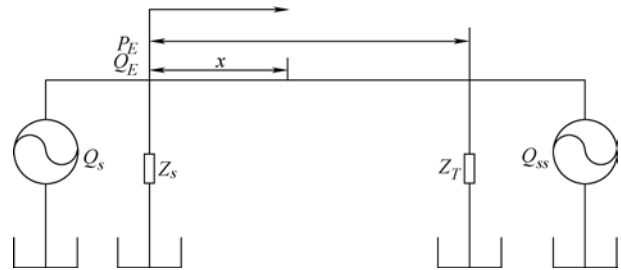


Fig. 5. Test principle of secondary source method

The Secondary Source Method is based on the assumption that the source impedance and source flow ripple connects in parallel. The source flow can be computed by the following equations<sup>[13–14]</sup>:

$$Q_s = Q_E + \frac{P_E}{Z_s} \quad (9)$$

Based on Eq. (9), it can be seen that the source impedance must be calculated firstly for computing the source flow ripple, and the test apparatus is shown in Fig. 6.

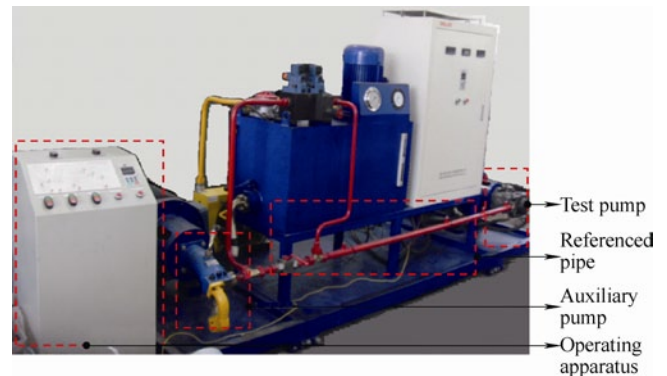


Fig. 6. Test apparatus of secondary source method

In the interest of validating the simulation model, the test and simulation results are obtained in the same operating condition: the pump suction pressure is set at 2MPa, the swash plate angle is 13°, the pump delivery pressure is set at 5 MPa, 10 MPa, 15 MPa, and the pump speed is 400  $\text{r} \cdot \text{min}^{-1}$ , 800  $\text{r} \cdot \text{min}^{-1}$  and 1 500  $\text{r} \cdot \text{min}^{-1}$  respectively.

The test pump is without PCV. The simulation and test results of flow ripple under different pump delivery pressure and pump speed are presented in Fig. 7.

From Fig. 7, it is easy to be seen that the simulation results agrees well with the test results under different pump delivery pressures and pump speeds. Firstly, the variation trends of these results are very similar to each

other. In addition, the levels of extreme values of these two results have small difference. More important, the non-uniformity grade of flow ripple and the mean flow rate are almost the same. Therefore it can be concluded that the simulation model is appropriate for serving as fundamental model of piston pump with PCV.

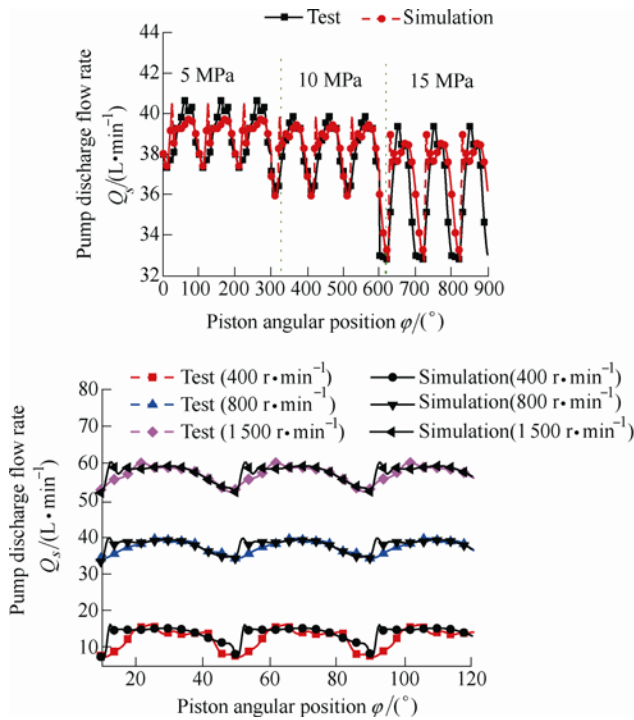


Fig. 7. Comparison between test and simulation results

### 3.2 Comparison with other publication results

#### 3.2.1 Pump delivery pressure

The simulation and experimental flow ripples under different pump delivery pressure given by PETTERSSON M. E. are shown in Fig. 8<sup>[15]</sup>.

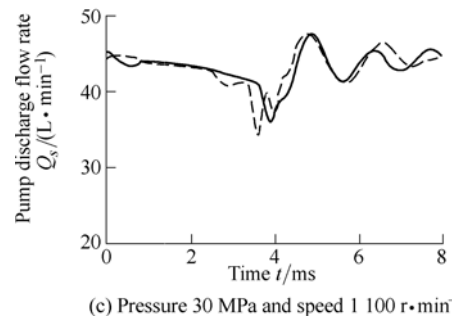
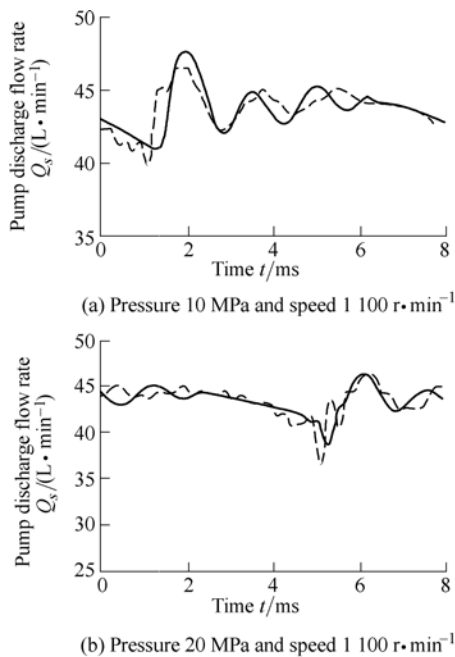


Fig. 8. Simulation(solid line) and experiment(dot line) source flow under different pump delivery pressure

It can be seen from Fig. 8 that the minimum value of the source flow rate decreases with the increase in pressure, and the simulation results and the experiment results match well. In addition, the maximum value of the source flow rate is almost the same with the increase of pressure.

The results obtained with the finite element method are shown in Fig. 9.

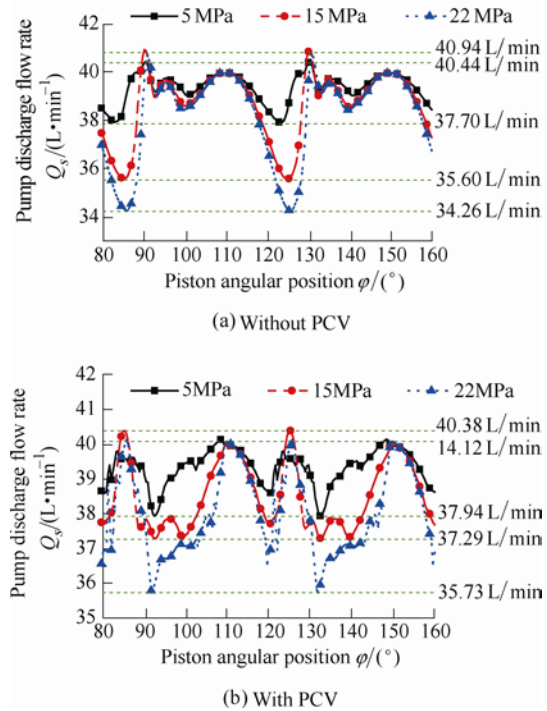


Fig. 9. Flow ripple obtained with finite element model under different pump delivery pressure

It is shown by Fig. 9(b) that the minimum flow rate decreases with the increase in pressure and the maximum flow rate is almost the same. Compared with Fig. 8, the variation trends of the source flow are the same, so it is reasonable to conclude that the finite element model can be used to analyze the source flow rate of the pump with PCV under different pressure.

It can also be seen from Fig. 9 that the minimum flow rate with PCV is bigger than the flow rate without PCV, the maximum flow rate, amplitude and non-uniformity grade of the flow ripples with PCV (according to the comparison of flow ripples with/without PCV) is smaller than those value

without PCV in all scale of pump delivery pressure. So it can be concluded that the PCV method can reduce flow ripple at large variation of pump delivery pressure.

### 3.2.2 Pump speed

The simulation and experimental flow ripples under different pump speed given by PETTERSSON M. E. are shown in Fig. 10<sup>[15]</sup>.

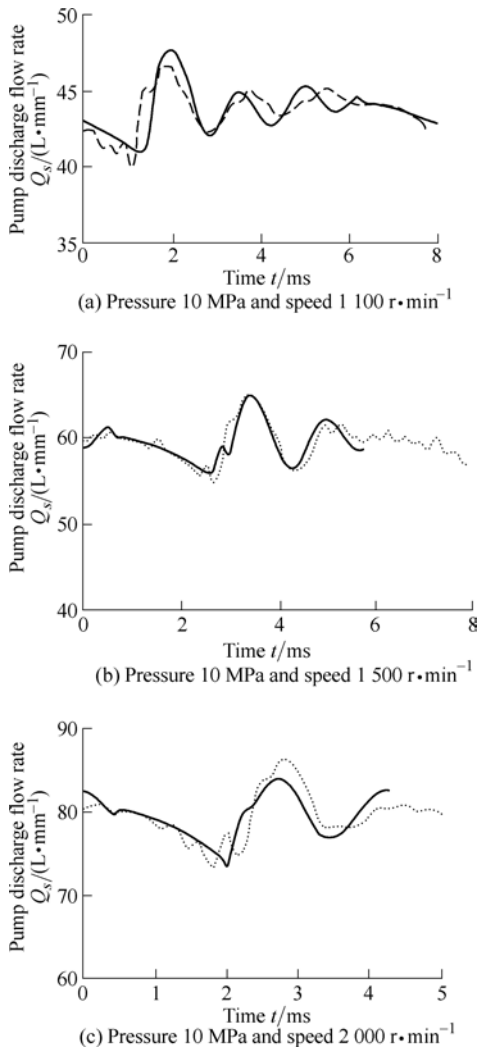


Fig. 10. Simulation(solid line) and experiment(dot line) source flow under different pump speed

It can be seen from Fig. 10 that the amplitude and mean value of the flow rate increase with the increase of pump speed.

The source flow rate obtained with finite element model under different pump speed is shown in Fig. 11.

It can be seen that the variation trends of the source flow rate with increasing pump speed in Fig. 11(b) is the same as in Fig. 10, so it can be concluded that the simulation model can be used to analyze the source flow rate under different pump speed.

Comparing the result of flow ripple with /without PCV in Fig. 11, the minimum flow rate with PCV is bigger than the one without PCV, and the maximum flow rate decreases after introducing the PCV in most pump speed except that

the maximum flow rate increases when the pump speed is 400 r·min<sup>-1</sup>. The amplitude, non-uniformity grade of flow ripple decreases after introducing PCV under different pump speed, so it can be concluded that the PCV method can reduce flow ripple when the pump speed is between 400 r·min<sup>-1</sup> and 1 500 r·min<sup>-1</sup>.

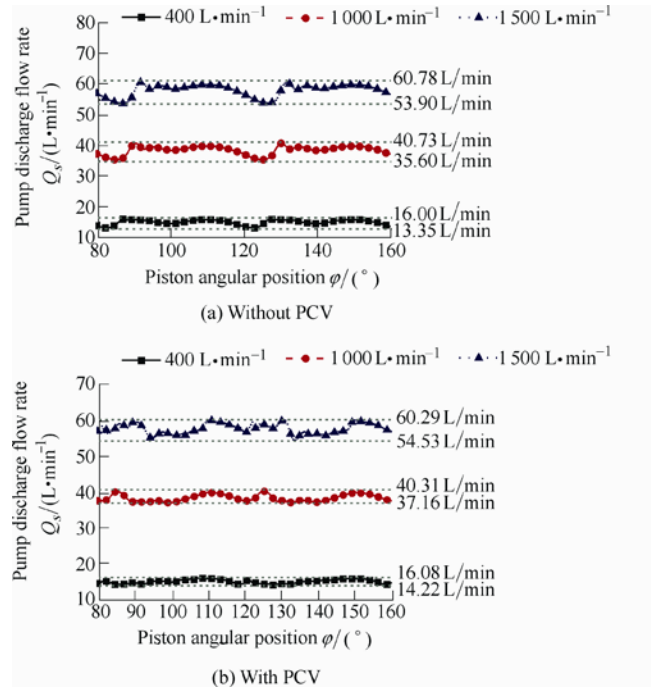


Fig. 11. Flow ripple obtained with finite element model under different pump speed

## 4 Results and Discussion of the Piston Pump Simulation Model

The optimizations of the PCV volume and angle are determined through simulation under typical operation condition, and then the effect of swash plate angle on flow ripple is provided.

### 4.1 Optimization of the PCV volume

The simulation model is solved under a typical condition when the pump delivery pressure is 15MPa, the pump suction pressure 2 MPa, pump speed 1 000 r·min<sup>-1</sup>, swash plate angle 13° and the PCV angle 15°. The comparison of flow ripples with different volumes of PCV (signed with V) is shown in Fig. 12.

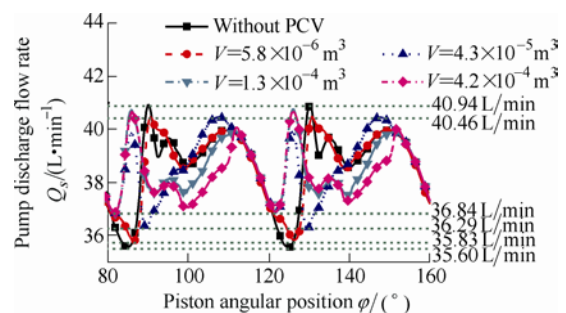


Fig. 12. Flow ripples under different PCV Volume

It can be seen from Fig. 12 and Table 2 that when the PCV Volume is  $4.2 \times 10^{-4} \text{ m}^3$ , the maximum flow rate decreases and the minimum flow rate increases the most, and the mean flow rate, amplitude and non-uniformity grade of flow ripple decreases the most. However, the ratio of the Non uniformity grade of flow ripple to PCV Volume (8.4, 5.6, 1.5), which is obtained from the results that the difference of Non-uniformity grade of flow ripple is divided by the difference of the PCV volume, is decreased greatly with the increasing PCV volume. In other words, when the PCV volume is more than  $1.3 \times 10^{-4} \text{ m}^3$ , the left space for reducing the Non-uniformity grade of the flow ripple is less than 10% with PCV method, it is not cost-effective to increase the PCV volume for reducing flow ripple of piston pump. So it can be concluded that the PCV volume with  $1.3 \times 10^{-4} \text{ m}^3$  is appropriate value for the piston pump.

**Table 2. Estimation parameters under different PCV volume**

Volume $V/\text{m}^3$	L/min				
	Max $\Delta Q_{\max}$	Min $\Delta Q_{\min}$	Mean $Q_m$	Amplitude $\Delta Q$	Non-uniformity grade $\delta/\%$
$5.8 \times 10^{-6}$	-1.11	0.66	-0.28	-12.90	-12.66
$4.3 \times 10^{-5}$	-1.16	1.96	0.29	-21.93	-22.15
$1.3 \times 10^{-4}$	-0.46	3.48	1.37	-26.80	-27.79
$4.2 \times 10^{-4}$	-0.66	3.64	1.34	-29.30	-30.23

**4.2 Optimization of the PCV volume**

The simulation model is solved when the pump operating conditions are the same with the operating conditions mentioned above and the PCV volume is  $1.3 \times 10^{-4} \text{ m}^3$ , the PCV angle is set at  $-15^\circ$ ,  $13^\circ$ ,  $15^\circ$ ,  $17^\circ$  respectively. The comparison of flow ripples with different angles of PCV (signed with A) is shown in Fig. 13.

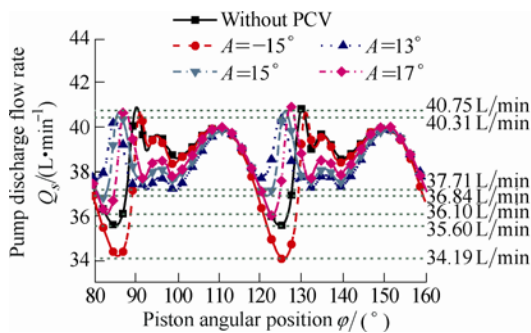


Fig. 13. Flow ripples under different PCV angle

Based on Fig. 13 and Table 3, it can be seen that when the PCV angle is  $13^\circ$ , the minimum flow rate and the mean flow rate increase the most; the maximum flow rate, the amplitude and the non-uniformity grade of flow ripple decrease the most.

When the PCV angle is between  $12^\circ$  to  $14^\circ$ , the minimum and maximum flow rate is shown in Fig. 14.

**Table 3. Estimation parameters under different PCV Angle**

Angle $A/(\circ)$	L/min				
	Max $\Delta Q_{\max}$	Min $\Delta Q_{\min}$	Mean $Q_m$	Amplitude $\Delta Q$	Non-uniformity grade $\delta/\%$
-15	-0.62	-3.95	-2.17	21.57	24.26
13	-1.52	5.95	1.95	-51.34	-52.27
15	-0.46	3.48	1.37	-26.79	-27.79
17	-0.51	1.41	0.38	-13.31	-13.64

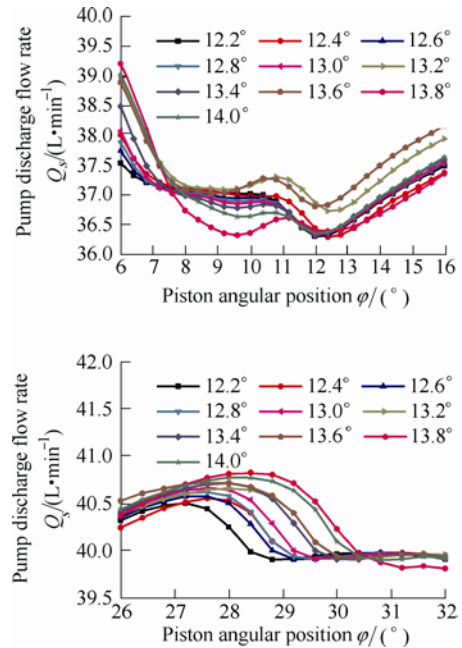


Fig. 14. Peak value under different PCV angle

From Fig. 14, it can be seen that when the PCV angle is  $13^\circ$ , the amplitude and the non-uniformity grade of flow ripple reaches the smallest, so it is convinced that the PCV angle with  $13^\circ$  is the best under such operating condition.

**4.3 Effect of swash plate angle**

When the PCV angle is  $13^\circ$  and the volume is  $1.3 \times 10^{-4} \text{ m}^3$ , the pump suction pressure 2 MPa, pump delivery pressure is 15 MPa, pump speed is 1 000 r/min, and the comparison of flow ripples with/without PCV under different swash plate angle ( $11^\circ$ ,  $13^\circ$ ,  $15^\circ$  and  $17^\circ$ ) is shown in Fig. 15.

It can be seen from Fig. 15 that the minimum flow rate with PCV is bigger than the one without PCV, and the maximum flow rate increases after introducing the PCV when the swash plate angle is between the  $11^\circ$  and  $17^\circ$ . Compared with the results without PCV, the amplitude and non-uniformity grade of flow ripple decrease under different swash plate. So it can be concluded that the PCV method can reduce flow ripple when the swash plate angle is between  $11^\circ$  and  $17^\circ$ .

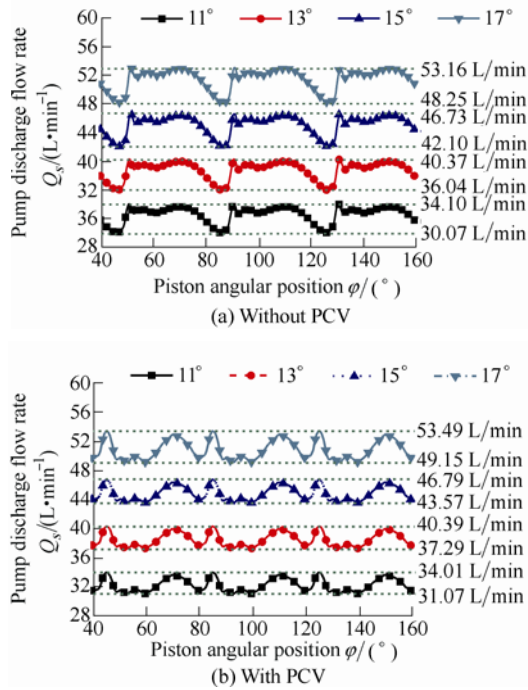


Fig. 15. Flow ripples under different swash plate angle

## 5 Conclusions

(1) The flow ripple can be reduced most with PCV angle  $13^\circ$ , PCV volume  $1.3 \times 10^{-4} \text{ m}^3$ , when the pump delivery pressure is 15MPa, pump suction pressure is 2MPa, pump speed is  $1000 \text{ r} \cdot \text{min}^{-1}$  and swash plate angle is  $13^\circ$ .

(2) With the PCV angle  $13^\circ$ , PCV volume  $1.3 \times 10^{-4} \text{ m}^3$ , this method can reduce flow ripple of the piston pump when the pump suction pressure is 2 MPa, the pump delivery pressure is 5 MPa, 15 MPa, 22 MPa, pump speed is  $400 \text{ r} \cdot \text{min}^{-1}$ ,  $1000 \text{ r} \cdot \text{min}^{-1}$ ,  $1500 \text{ r} \cdot \text{min}^{-1}$  and swash plate angle is  $11^\circ$ ,  $13^\circ$ ,  $15^\circ$  and  $17^\circ$  respectively.

(3) The finite element simulation model of the piston pump can be used in optimizing the PCV structure and guiding for design of a quieter axial piston pump.

## References

- [1] MANRING Noah D, ZHANG Yihong. Valve-plate design for an axial piston pump at low displacement[J]. *Journal of Mechanical Design, Transaction of the ASME*, 2003, 125: 200–207.
- [2] IVANTYSNOVA Monika, HUANG Changchun, CHRISTIANSEN Sven-kelana. Computer aided valve plate design-an effective way to reduce noise[J]. *SAE International*, 2004: 78–90.
- [3] MANRING Noah D, DONG Zhilin. The impact of using a secondary swash-plate angle within an axial piston pump[J]. *Journal of Dynamic Systems, Measurement And Control*, 2004, 126: 67–74.
- [4] ERICSON Liselott. *Measurement system for hydrostatic pump flow pulsations*[D]. Linköping: Linköping University, 2005.

- [5] WANG Lin. *Active control of fluid-borne noise*[D]. Bath: University of Bath, 2008.
- [6] TIMO Nafz, HUBERTUS Murrenhoff, RUSIAN Rudik. Active systems for noise reduction and efficiency improvement of axial piston pumps[C]//*Proceeding of Fluid Power and Motion Control*, Bath: PTMC, 2008: 327–340.
- [7] PETTERSSON M E, WEDDFELT K G, PALMBERG J S. Methods of reducing flow ripple from fluid power pumps—a theoretical approach[J]. *SAE Technical Paper Series*, 1991, (911762): 1–10.
- [8] SEENIRAJ Ganesh Kumar, IVANTYSNOVA Monika. Noise reduction in axial piston machines based on multi-parameter optimization[C]//*Proceeding of 4th FPNI-PhD Symposium*, Sarasota 2006: 235–246.
- [9] MEHTA Viral. *Torque ripple attenuation for an axial piston swash plate type hydrostatic pump: noise consideration*[D]. Columbia, University of Missouri-Columbia, 2006.
- [10] XU Bing, ZHANG Junhui, YANG Huayong, et al. Investigation on the radial micro-motion about piston of axial piston pump[J]. *Chinese Journal of Mechanical Engineering*, 2013, 26(2): 325–333.
- [11] ZHANG Bin, XU Bing, XIA Chunlin, et al. Modeling and simulation on axial piston pump based on virtual prototype technology[J]. *Chinese Journal of Mechanical Engineering*, 2009, 22(1): 84–90.
- [12] MA Jien. *Study on Flow ripple and valve plate optimization of axial piston pump*[D]. Hangzhou: Zhejiang University, 2009.
- [13] MA Jien, XU Bing, ZHANG Bin, et al. Study on flow ripple of axial piston pump with CFD simulation using compressible fluid oil[J]. *Chinese Journal of Mechanical Engineering*, 2010, 23(1): 45–52.
- [14] The International Organization for Standardization. *ISO 10767-1-1996 Hydraulic Fluid Power-Determination of Pressure Ripple Levels Generated in System and Components Part 1: Precision method for pumps*[S]. London: British Standards Institution, 1996.
- [15] PETTERSSON M E. *Design of fluid power piston pumps with special reference to noise reduction*[D]. Linköping: Linköping University, 1995.

## Biographical notes

XU Bing, born in 1971, is a professor at *State Key Lab of Fluid Power and Mechatronic System, Zhejiang University, China*. His main research interests include mechatronics engineering, fluid power element and system.  
E-mail: bxu@zju.edu.cn

SONG Yuechao, born in 1981, obtained her PhD degree at *Zhejiang University, China*, in 2013. Her research interests include fluid power element.  
E-mail: syc19810807@sina.com

YANG Huayong, born in 1961, is currently a professor and a PhD candidate supervisor at *State Key Lab of Fluid Power and Mechatronic System, Zhejiang University, China*. His main research interests include mechatronics engineering, fluid power transmission and control.  
E-mail: yhy@zju.edu.cn